On the role of surface shape in a micro-scale heat conduction problem

A Dinler, I Graur, R Barber, D R Emerson, P Perrier

On the role of surface shape in a micro-scale heat conduction problem

2012 J. Phys.: Conf. Ser. 362 012017

(http://iopscience.iop.org/1742-6596/362/1/012017)

On the role of surface shape in a micro-scale heat conduction problem

A Dinler[1*], I A Graur[2], R W Barber[1], D R Emerson[1] and P Perrier[2]

[1] Centre for Microfluidics and Microsystems Modelling, STFC Daresbury Laboratory, Warrington WA4 4AD, United Kingdom
[2] Universite de Provence, Ecole Polytechnique Universitaire de Marseille, UMR CNRS 6595, 5 rue Enrico Fermi, 13453 Marseille, France

Abstract. The present study investigates the importance of the surface shape in a micro-scale heat conduction problem. A heated infinitely-thin cylindrical shell is positioned in the middle of two concentric cylinders, and the heat transfer through a rarefied gas between the shell and the confining inner (or outer) cylinder is investigated. The study initially considers the solution of the first- and second-order temperature-jump models (*i.e.* the conventional heat equation with temperature-jump boundary conditions). The study then examines the numerical solution of the nonlinear Shakhov model kinetic equation subject to the Maxwell boundary condition using the discrete velocity method (DVM). The variable-hard-sphere molecular interaction model is taken into account in the temperature-jump models allowing the presence of significant temperature differences between surfaces to be considered. Anomalous temperature profiles near the convex (or concave) side of the shell are attributed to the effects of surface shape.

1. Introduction

Understanding the role of heat flow is an essential part of designing various MEMS and NEMS devices. Several microelectronic devices are exposed to a significant quantity of heat in operation, while many microdevices are based on heat transfer phenomena such as thermoelastic actuators and thermal anemometers [1,2]. Some other MEMS devices are designed to enhance the heating or cooling performance by incorporating more complex manifold geometries. However, the role of surface shape and curvature in the heat transfer between a microsystem and its environment has not been fully understood.

The present study investigates the importance of the surface shape in micro-scale heat conduction around an infinitely-thin cylindrical shell. A heated cylindrical shell is positioned in the middle of two concentric cylinders, and the heat transfer through a rarefied gas between the shell and the confining inner (or outer) cylinder is investigated. Since the shell has both concave and convex sides with the same surface area and same degree of curvature, any anomalous behaviour in the heat flow over the concave or convex side can be attributed directly to the effects of surface shape. The study initially considers the solution of the first- and second-order temperature-jump models (*i.e.* the conventional heat equation with temperature-jump boundary conditions) by taking into account the presence of significant temperature gradients. Then, the study examines the numerical solution of the nonlinear

* ali.dinler@stfc.ac.uk Tel: +44 (0)1925 603663

Shakhov model kinetic equation subject to the Maxwell boundary condition using the discrete velocity method (DVM).

The present study reveals the remarkable effects of the surface shape and curvature. The results show that the degree of temperature jump over a convex surface is markedly larger than that over a concave surface. The results clearly demonstrate the difference in the magnitudes of the heat fluxes over the concave and convex surfaces of the shell. The present study also investigates the accuracy of temperature-jump models over nonplanar surfaces in comparison with both the solution of the nonlinear Shakhov model kinetic equation and direct simulation Monte Carlo (DSMC) results. The DSMC data and the nonlinear Shakhov kinetic solution are found to be in excellent agreement for the cases considered in this study.

2. Continuum description of the problem

The present study considers a heated infinitely-thin cylindrical shell positioned in the middle of a gap between two concentric cylinders. The energy equation for the heat transfer through a rarefied gas between the shell and the confining inner (or outer) cylinder can be written in a cylindrical-polar coordinate reference frame as

$$\frac{\partial}{\partial r}\left[k(T)\frac{\partial T}{\partial r} r \right] = 0 \tag{1}$$

where T is the temperature and r is the radial distance. The thermal conductivity $k(T)$ depends on temperature T with a variable hard sphere (VHS) power law $k(T) = k_0 (T/T_0)^{\omega}$, where T_0 is the reference temperature and k_0 is the thermal conductivity at T_0. In the presence of a significant temperature difference between the surface and its environment (*i.e.* in the presence of significant temperature gradients), the variable hard sphere power law must be taken into account in the modelling. The exponent, ω, typically lies in the range between 0.5 (for hard sphere molecules) and 1 (for Maxwell molecules).

The general solution of equation (1) is given by

$$T(r) = (\omega+1)\left[C_1 + C_2 T_0^{\omega} \ln r \right]^{1/(\omega+1)} \tag{2}$$

where C_1 and C_2 are the constants determined by the temperature-jump boundary conditions. The heat flux can then be written as

$$q(r) = -k(T)\frac{dT}{dr} = -\frac{k_0}{r}\left[C_2 \Sigma^{-1+1/(\omega+1)} (1+\omega)^{\omega} \Sigma^{\omega/(\omega+1)} \right] \tag{3}$$

where $\Sigma = C_1 + C_2 T_0^{\omega} \ln r$.

Several first- and second-order temperature-jump boundary conditions are proposed in the literature for modelling the heat transfer over planar surfaces, as reviewed by Colin [3]. The temperature-jump solutions for the planar geometry are reported to be in good agreement with DSMC data up to a Knudsen number of 0.4 [4]. However, relatively little research has been conducted on their accuracy at nonplanar surfaces. The Knudsen number can be defined in terms of the annular gap between the shell and the confining inner (or outer) cylinder, *i.e.* $Kn = 2\lambda/(R_2 - R_1)$, where R_1 and R_2 are the radii of the inner and outer cylinders, and λ is the mean free path, defined as $\lambda = (\mu/p)(\pi \bar{\mathrm{R}} T_0/2)^{1/2}$ where p is the pressure, μ is the dynamic viscosity and $\bar{\mathrm{R}}$ is the specific gas constant. When the mean free path is considered to be globally constant throughout the annular gap, the Knudsen number can be interpreted as a scale parameter which increases monotonically down to the micro/nanoscale.

The second-order temperature-jump boundary condition can be written as

$$T_{jump} = T_{gas} - T_{wall} = \frac{2-\sigma_T}{\sigma_T}\frac{2\gamma}{(\gamma+1)\mathrm{Pr}}\left(\pm\lambda\left.\frac{\partial T}{\partial n}\right|_{wall} - \frac{\lambda^2}{2}\left.\frac{\partial^2 T}{\partial n^2}\right|_{wall}\right) \tag{4}$$

where σ_T is the thermal accommodation coefficient, γ is the specific heat ratio, Pr is the Prandtl number and $\partial/\partial n$ is the derivative in the direction normal to the surface. The specific heat ratio, γ, is assumed to be 5/3 and the Prandtl number, Pr, is taken as 2/3 whilst the thermal accommodation coefficient is specified as $\sigma_T = 1.0$ [5]. We employ a second-order temperature-jump boundary condition with a minus sign in front of the second term of order λ^2 in equation (4), instead of the positive sign originally proposed by Karniadakis *et al.* [6]. The first-order temperature jump condition can be obtained by omitting the second term in equation (4).

The solution of equation (2) can be found in the continuum regime for $T(R_1) = T_1$ and $T(R_2) = T_2$ as

$$T_{cont}(r) = (1+\omega)\left[\frac{T_1(T_1/(1+\omega))^{\omega}\ln(r/R_2) - T_2(T_2/(1+\omega))^{\omega}\ln(r/R_1)}{(1+\omega)\ln(R_1/R_2)}\right]^{1/(1+\omega)} \tag{5}$$

and the heat flux is given as

$$q_{cont}(r) = -k_0\frac{(1+\omega)^{\omega-1}\left[T_2(T_2/(1+\omega))^{\omega} - T_1(T_1/(1+\omega))^{\omega}\right]}{rT_0^{\omega}\ln(R_2/R_1)}. \tag{6}$$

When equation (2) is subjected to temperature-jump conditions, the constants C_1 and C_2 cannot be obtained straightforwardly. These constants are obtained numerically using a technique for the solution of the system of nonlinear equations. The exponent, ω, is set to 0.5 (*i.e.* hard sphere molecules) unless otherwise stated.

3. Formulation of the problem by the nonlinear Shakhov kinetic model

For the heat conduction problem through a rarefied gas between the heated shell and confining (cold) cylinder, the nonlinear Shakhov model kinetic equation is solved numerically and compared with first- and second-order temperature-jump models. The nonlinear Shakhov model kinetic equation is obtained by replacing the problematic collision term of the Boltzmann equation by a simpler collision model [7,8]. The Shakhov model is generally accepted to be more accurate for flows associated with heat transfer compared to the BGK (Bhatnagar, Gross and Krook) model, since the BGK model gives an incorrect Prandtl number equal to unity (*i.e.* Pr=1) instead of Pr=2/3 for monatomic gases [9,10]. In the present study, the Maxwell (specular/diffusive) boundary condition has been employed with the nonlinear Shakhov kinetic equation. It is important to note that the Boltzmann equation describes gas behaviour for all flow regimes and it is valid at all Knudsen numbers. The relation between the microscopic and macroscopic descriptions of gas is postulated as follows: all macroscopic quantities such as density, velocity and temperature are described in terms of the microscopic states, which are the solution of the Boltzmann equation. The state of the gas is given by the distribution function $f(\mathbf{x},\mathbf{v},t)$, where $\mathbf{x}$ is the position vector and $\mathbf{v}$ is the velocity vector of a molecule at time *t*. Once the distribution function is known, all the moments, for example gas density, pressure or heat flux can be computed.

By taking into account the axial symmetry of the shell problem problem in cylindrical coordinates (r,φ,z) in physical space, and considering the cylinders to be long enough to neglect the effects in the *z*-direction, the Shakhov model kinetic equation (*i.e.* the Boltzmann equation with the Shakhov collision model) can be written at steady-state as [10-12]

$$v_p \cos\theta \frac{\partial f}{\partial r} - \frac{v_p \sin\theta}{r} \frac{\partial f}{\partial \theta} = \frac{(f^S - f)}{\bar{\tau}} \tag{7}$$

using $v_r = v_p \cos\theta$, $v_\theta = v_p \sin\theta$ with $v_p = \sqrt{v_r^2 + v_\varphi^2}$ and $\theta = \arctan(v_\varphi / v_r)$, where the distribution function does not depend on φ (*i.e.* $\partial f / \partial \varphi = 0$) due to the axial symmetry. The term on the right-hand side of equation (7) is the Shakhov collision model

$$Q_S(f, f^S) = \frac{(f^S - f)}{\bar{\tau}} \tag{8}$$

where $\bar{\tau} = \mu / p$ is the relaxation time, μ is the dynamic viscosity and p is the gas pressure, and

$$f^S(r, \mathbf{v_c}) = f^M(r, \mathbf{v_c}) \left[1 + \frac{4m}{15 n(r) (k_B T(r))^2} q(r) v_p \cos\theta \left(\frac{m \mathbf{v_c}^2}{2 k_B T(r)} - \frac{5}{2} \right) \right] \tag{9}$$

with

$$f^M(r, \mathbf{v_c}) = n(r) \left(\frac{m}{2\pi k_B T(r)} \right)^{3/2} \exp\left(- \frac{m \mathbf{v_c}^2}{2 k_B T(r)} \right) \tag{10}$$

where $\mathbf{v_c}$ is the molecular velocity vector, r is the radial distance, f^M is the local Maxwellian distribution, m is the molecular mass, k_B is the Boltzmann constant, $q(r)$ is the heat flux profile in the radial direction, and $n(r)$ and $T(r)$ are the macroscopic number density and temperature profiles, respectively.

The unknown distribution function, f, in equation (7) depends on four variables (three velocity components and the radial distance). Collisions occur in this four dimensional phase space. However, the dependence of the distribution function on the velocity in the z-direction can be eliminated using a projection procedure. The reduced distribution functions ϕ and ψ are introduced [13] as

$$\phi(r, v_p, \theta) = \int f(r, \mathbf{v_c}) dv_z \text{ and } \psi(r, v_p, \theta) = \int f(r, \mathbf{v_c}) v_z^2 dv_z . \tag{11}$$

The dimensionless variables in the present study are specified as

$$\hat{r} = \frac{r}{R_2}, \quad \hat{T} = \frac{T}{T_2}, \quad \hat{\mathbf{v}} = \frac{\mathbf{v}}{v_0}, \quad \hat{n} = \frac{n}{n_0}, \quad \hat{p} = \frac{p}{p_2}, \quad \hat{\mu} = \frac{\mu}{\mu_2} = \hat{T}^\omega, \quad \hat{f} = \frac{f v_0^2}{n_0}, \quad \hat{q} = \frac{2}{n_0 m v_0^2} q \tag{12}$$

where $v_0 = \sqrt{2 k_B T_2 / m}$ is the most probable molecular velocity at T_2 and n_0 is the average numerical density, which is

$$n_0 = \frac{2}{R_2^2 - R_1^2} \int_{R_1}^{R_2} n(r) r dr . \tag{13}$$

The rarefaction parameter is defined as $\delta = R_2 p_2 / (\mu_2 v_0)$ where μ_2 is the dynamic viscosity at T_2. According to equations (12) and (13), the rarefaction parameter can be related to the Knudsen number as $\delta = \sqrt{\pi} R_2 / (2Kn(R_2 - R_1))$, where the rarefaction parameter is inversely proportional to the Knudsen number.

Multiplying equation (7) by 1 and v_z^2 , and integrating over v_z according to the relations in equation (11), two reduced kinetic equations are obtained in terms of the reduced distribution functions as

$$\hat{v}_p \cos\theta \frac{\partial \phi}{\partial \hat{r}} - \frac{\hat{v}_p \sin\theta}{\hat{r}} \frac{\partial \phi}{\partial \theta} = \delta \hat{n} \hat{T}^{1-\omega} (\phi^S - \phi) \tag{14}$$

$$\hat{v}_p \cos\theta \frac{\partial \psi}{\partial \hat{r}} - \frac{\hat{v}_p \sin\theta}{\hat{r}} \frac{\partial \psi}{\partial \theta} = \delta \hat{n} \hat{T}^{1-\omega} (\psi^S - \psi) \tag{15}$$

where

$$\phi^S = \phi^M \left[1 + \frac{4}{15} \frac{1}{\hat{n}\hat{T}^2} q(\hat{r}) \hat{v}_p \cos\theta \left(\frac{\hat{v}_p^2}{\hat{T}} - 2 \right) \right] \tag{16}$$

$$\psi^S = \psi^M \left[1 + \frac{4}{15} \frac{1}{\hat{n}\hat{T}^2} q(\hat{r}) \hat{v}_p \cos\theta \left(\frac{\hat{v}_p^2}{\hat{T}} - 1 \right) \right] \tag{17}$$

with

$$\phi^M = \frac{\hat{n}}{\pi \hat{T}} \exp\left(-\frac{\hat{v}_p^2}{\hat{T}} \right), \quad \psi^M = \frac{\hat{T}}{2} \phi^M, \quad \text{and} \quad \hat{v}_p^2 = \hat{v}_r^2 + \hat{v}_\theta^2. \tag{18}$$

The macroscopic quantities can be found in terms of the reduced distribution functions, ϕ and ψ, as [10-12]

$$\hat{n}(\hat{r}) = \int_0^{2\pi} \int_0^{\infty} \phi \hat{v}_p d\hat{v}_p d\theta \tag{19}$$

$$\hat{T}(\hat{r}) = \frac{2}{3\hat{n}(\hat{r})} \int_0^{2\pi} \int_0^{\infty} (\hat{v}_p^2 \phi + \psi) \hat{v}_p d\hat{v}_p d\theta \tag{20}$$

$$\hat{q}(\hat{r}) = \frac{2}{3\hat{n}(\hat{r})} \int_0^{2\pi} \int_0^{\infty} (\hat{v}_p^2 \phi + \psi) \hat{v}_r \hat{v}_p d\hat{v}_p d\theta \tag{21}$$

with the equation of state $p = nk_B T$.

The present study implements the Maxwell (specular/diffusive) gas-wall interaction model. In the Maxwell model, a proportion of the molecules, α, are reflected diffusively from the surface while the remaining proportion, $1-\alpha$, are reflected specularly from the surface. The specular reflection model is straightforward. When a molecule strikes a wall, the normal velocity component of the molecule is simply reversed and directed back into the flow domain; the other velocity components remain unchanged. In other words, the molecules bounce off the wall with the same velocity distribution except their reversed normal velocity components, while their other velocity components remain unchanged. For the diffuse reflection, the reflected tangential velocity of the molecule is considered to be uncorrelated with its impinging velocity and the molecules bounces off the surface according to the local Maxwell distribution. Therefore, for equation (14), the Maxwell boundary conditions at the inner and outer cylinders can be written as

$$\phi(r_1, \hat{v}_p, \theta) = (1-\alpha)\phi(r_1, \hat{v}_p, \pi - \theta) + \alpha \frac{n_1}{\pi \hat{T}_1} \exp\left(-\frac{\hat{v}_p^2}{\hat{T}_1} \right), \quad -\pi/2 \le \theta \le \pi/2 \tag{22}$$

$$\phi(1, \hat{v}_p, \theta) = (1-\alpha)\phi(1, \hat{v}_p, \pi - \theta) + \alpha \frac{n_2}{\pi} \exp(-\hat{v}_p^2), \quad \pi/2 \le \theta \le 3\pi/2 \tag{23}$$

associated with impermeability assumption [10]:

$$n_1 = 2\sqrt{\frac{\pi}{\hat{T}_1}} \int_0^{\infty} \hat{v}_p^2 d\hat{v}_p \int_{-\pi/2}^{\pi/2} \phi \cos\theta d\theta \quad \text{and} \quad n_2 = -2\sqrt{\pi} \int_0^{\infty} \hat{v}_p^2 d\hat{v}_p \int_{\pi/2}^{3\pi/2} \phi \cos\theta d\theta \tag{24}$$

where $0 \le \alpha \le 1$ is the accommodation coefficient, $r_1 = R_1/R_2$ is the ratio between cylinder radii and $\hat{T}_1 = T_1/T_2$ is the ratio between the inner and outer cylinder temperatures. The boundary conditions for equation (15) can be written in a very similar manner. In the present study, the accommodation coefficient, α, is specified as unity (*i.e.* $\alpha = 1$), and therefore only fully diffusive reflections are considered.

The heat transfer problem under consideration is solved using a computational scheme that discretizes equation (14) (and equation (15) in a similar manner) into

$$v_{p_k} \cos\theta_m \frac{\phi^j_{i,k,m} - \phi^j_{i-\beta,k,m}}{\beta \Delta \hat{r}} - v_{p_k} \frac{\sin\theta_m}{\hat{r}_i} \frac{\phi^j_{i,k,m} - \phi^j_{i,k,m-1}}{\Delta\theta} = \delta \hat{n}_i^{j-1} (\hat{T}_i^{1-\omega})^{j-1} ((\phi^S_{i,k,m})^{j-1} - \phi^j_{i,k,m}) \qquad (25)$$

where i and m are the indices in the r and θ directions, respectively, j is the iteration index, $\beta = sign(\cos\theta_m)$ is the sign of $\cos\theta_m$; and k is the index for the Gauss quadrature points. In the present study, the annular clearance between the cylinders $[R_1/R_2, 1]$ and the angular period $[0, \pi]$ are divided into 100 equal intervals. For the velocity space, the magnitudes of the molecular velocity, c_{p_k}, are mapped onto 20 Gauss quadrature points with their associated weights. Integrals (19)-(21) for calculating the macroscopic quantities are obtained using the Gauss quadrature rule at each iteration. When the difference between macroscopic temperatures of successive iterations is smaller than a certain tolerance value, the convergence criterion is assumed to be fulfilled.

4. Results and discussions

The second-order temperature profiles of the shell problem are shown in figure 1. The temperature-jump models predict the profound effects of the surface shape (*i.e.* convex/concave) on the degree of temperature jump. The bold vertical lines in the middle of the figures represent the location of the shell. The profiles on the left (blue) and right (red) sides of the shell are created by the concave and convex sides of the heated shell, and they have obviously identical curvatures and surface areas. The remarkable differences in the degrees of temperature jump are attributed to the effects of surface shape. Figure 1 clearly reveals the role of the surface shape, since the degrees of temperature jump would be equal on both sides of the shell in an equivalent geometry between parallel plates.

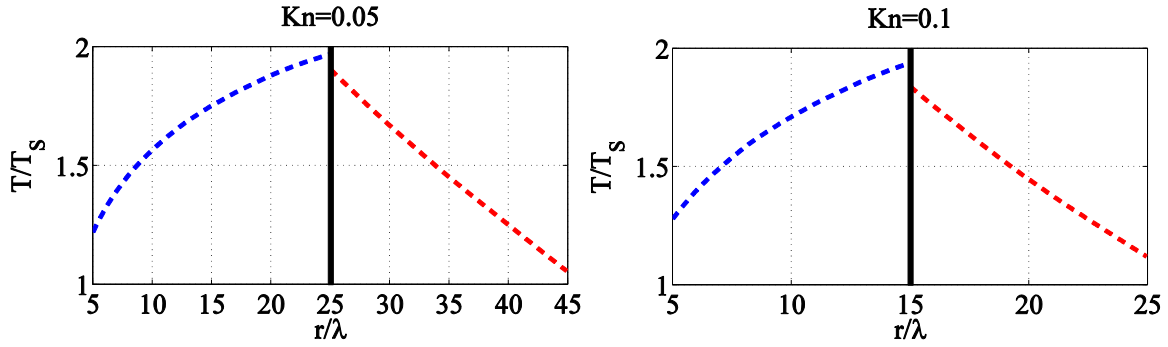

Figure 1. Second-order temperature profiles over the concave and convex surfaces of a heated cylindrical shell. The profiles on the left (blue) and right (red) sides of the shell are created by the concave and convex shell surfaces, respectively. The shell is positioned midway between two cold cylinders and it has a radius of (a) 25λ and (b) 15λ, where λ is the mean free path. The ratio of the temperature of the shell to the temperature of the inner (or outer) cylinder is 2. (a) *Kn*=0.05 and (b) *Kn*=0.1.

The effect of the Knudsen number on the temperature jumps over the concave and convex surfaces of the heated cylindrical shell are demonstrated in figure 2. The temperature jumps are obtained from first- and second-order jump models and the nonlinear Shakhov model solution. Figure 2 presents the results in terms of the Knudsen number where the corresponding rarefaction parameter can be identified using the formula $\delta = \sqrt{\pi} R_2 / (2Kn(R_2 - R_1))$. According to this formulation, the rarefaction parameter is $\delta_{convex} = \sqrt{\pi} R_2 / (2Kn(R_2 - R_S))$ on the convex side, whilst it is $\delta_{concave} = \sqrt{\pi} R_S / (2Kn(R_S - R_1))$ on the concave side of the shell, where R_S the radius of the shell. Therefore, the rarefaction parameter is slightly higher (*i.e. Kn* is slightly lower) on the convex side of the shell; in fact, this supports our important conclusions about the significant effects of curvature.

In figure 2, the concave and convex sides of the shell have the same surface area and same degree of curvature. The results remarkably show that the degree of temperature jump over a convex surface is markedly larger than that over a concave surface. Moreover, the jump models predict the amount of temperature jump relatively well up to *Kn*=0.3. However, beyond *Kn*=0.3, the predictions of the temperature-jump models start to deviate from the nonlinear Shakhov model solution. Figure 2 also shows that the second order jump solution is slightly in better agreement with the solution of nonlinear Shakhov model equation compared to the first-order solution in predicting the amount of temperature jump over the shell.

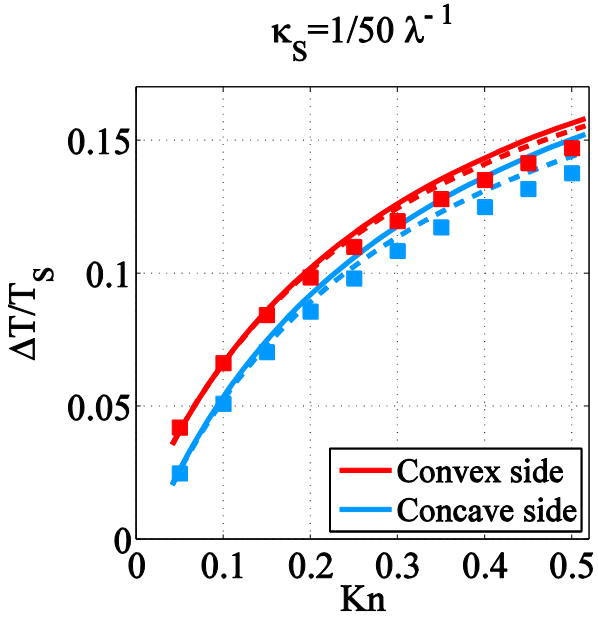

Figure 2. Temperature jumps over the concave and convex surfaces of a heated cylindrical shell against the Knudsen number. The red and blue curves illustrate temperature jumps over the convex and concave sides of the shell, respectively. The solid and dashed curves are the first- and second-order temperature-jump solutions, respectively. The square symbols illustrate the temperature jumps obtained from the solution of nonlinear Shakhov model kinetic equation. The shell curvature is $\kappa_S = 1/50\lambda^{-1}$ (*i.e.* the shell radius is $R_S = 50\lambda$).

Figure 3 shows that the DSMC data and the nonlinear Shakhov model solution are in excellent agreement. On the other hand, the accuracy of temperature-jump models deteriorates when the cylinder surface is cooler than the surrounding gas. This has been reported before for the planar heat conduction problem by Pan *et al.* [14] when trying to determine the temperature-jump coefficient of a first-order temperature-jump boundary condition. Using the DSMC method, Pan *et al*. [14] deduced different coefficients for the heat flow from a hot gas to a colder wall compared to the heat flow from a hot wall to a colder gas.

The magnitudes of the heat fluxes over the concave and convex surfaces of the shell are demonstrated in figure 4. The profiles are obtained from the solution of the nonlinear Shakhov model kinetic equation. The shell curvature is $\kappa_S = 1/6\lambda^{-1}$ (*i.e.* the shell radius is $R_S = 6\lambda$). The results remarkably show the dramatic effect of the surface shape on the heat flux; the heat flux is significantly higher over the convex surface compared to the concave surface of the shell.

The variation of the normalized heat fluxes over the concave and convex surfaces are shown in figure 5 for increasing values of curvature of the shell. The heat fluxes are obtained from the first-order temperature-jump model and normalized by the heat flux of the continuum regime as obtained in equation (6). For Knudsen numbers of 0.05 and 0.1, the first and second-order order jump solutions are expected to be very close to each other. Figure 5 shows that, as the curvature of the shell increases, the heat fluxes over the concave and convex surfaces of the shell start to show significant differences. It can be seen that the heat flux over the concave side becomes considerably lower than the heat flux over the convex side of the shell, beyond a certain curvature value depending on the Knudsen number.

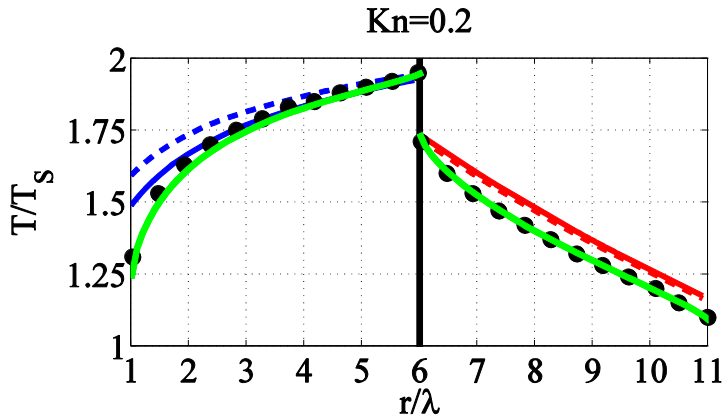

Figure 3. Temperature profiles over the concave and convex surfaces of the heated cylindrical shell. The profiles on the left- and right-hand sides of the shell are created by the heated concave and convex shell surfaces, respectively. The red and blue curves illustrate the temperature profiles obtained from the jump models over the convex and concave sides of the shell, respectively. The solid and dashed curves are the first- and second-order temperature-jump solutions, respectively. The green curves illustrate the temperature profiles obtained from the solution of nonlinear Shakhov model kinetic equation. The black dots are the DSMC data.

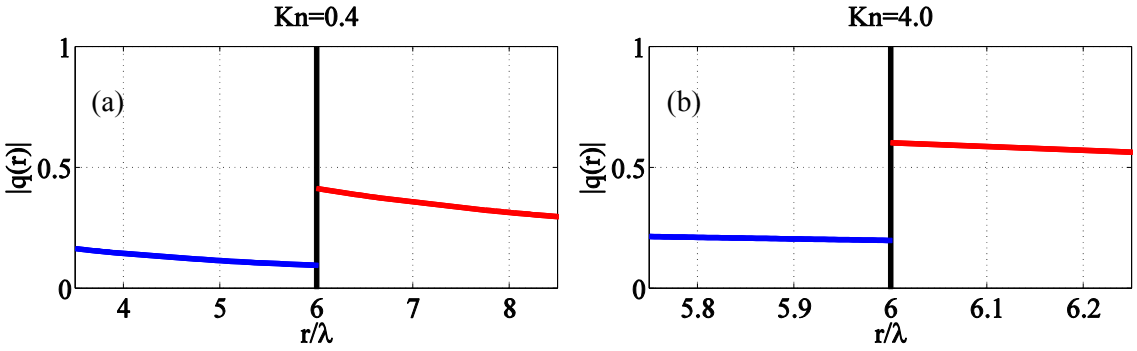

Figure 4. Magnitudes of the heat fluxes in the radial direction over the concave and convex surfaces of the shell. The profiles are obtained from the solution of the nonlinear Shakhov model kinetic equation. (a) *Kn*=0.4, (b) *Kn*=4.0.

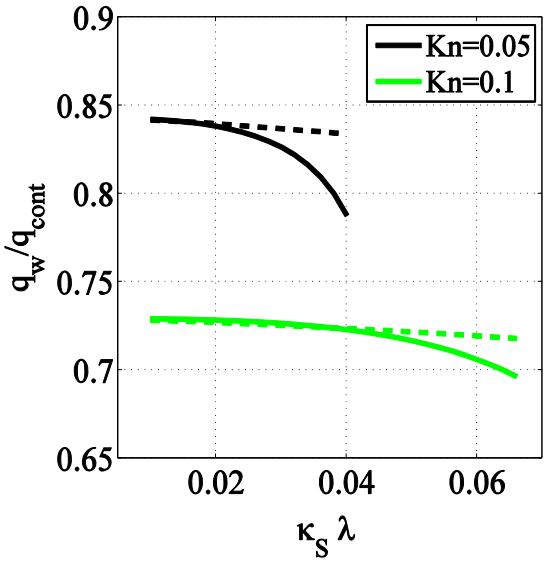

Figure 5. Normalized heat fluxes at the shell surface predicted by the first-order temperature-jump model against the curvature of the shell. The dashed and solid curves are the heat fluxes over the convex and concave surfaces of the shell, respectively, and q_{cont} is the heat flux in the continuum regime as $\mathrm{Kn} \to 0$.

Acknowledgments
The authors would like to thank Manual Vargas and Stefan Stefanov from the Institute of Mechanics, Bulgarian Academy of Sciences, for allowing the authors to use their DSMC code. The first author would also like to thank Irina Graur and Pierre Perrier for their warm welcome during his stay in Marseille. The research leading to these results has received funding from the European Community's Seventh Framework Programme (ITN - FP7/2007-2013) under the GASMEMS project with a grant agreement no: 215504.

References
[1] Pelesko J A and Bernstein D H 2003 *Modeling MEMS and NEMS* (Boca Raton, FL: Chapman & Hall/CRC)
[2] Nguyen N -T and Wereley S T 2006 *Fundamentals and Applications of Microfluidics* (Boston: Artech House)
[3] Colin S 2012 *Journal of Heat Transfer* **134** 020908
[4] Wadsworth D C 1993 *Phys. Fluids A* **5** 1831
[5] Sharipov F 2011 *J. Phys. Chem. Ref. Data* **40** 023101
[6] Karniadakis G E, Beskok A and Aluru N 2005 *Microflows and Nanoflows: Fundamentals and Simulation* (Berlin: Springer)
[7] Chu C K 1965 *Phys. Fluids* **8** 12
[8] Shakhov E M 1968 *Fluid Dynamics* **3** 156
[9] Shakhov E M 1968 *Fluid Dynamics* **3** 142
[10] Graur I A and Polikarpov A P 2009 *Heat Mass Transfer* **46** 237
[11] Sharipov F and Bertoldo G 2006 *J. Vac. Sci. Technol. A* **24** 2087
[12] Pantazis S and Valougeorgis D 2010 *Eur. J. Mech. B/Fluids* **29** 494
[13] Zhuk V I, Rykov V A and Shakhov E M 1973 *Fluid Dynamics* **8** 620
[14] Pan L S, Ng T Y, Xu D, Liu G R and Lam K Y 2002 *J. Micromech. Microeng.* **12** 41